THE JOURNAL OF PHYSICAL CHEMISTRY B

Article

pubs.acs.org/JPCB

Photochromism of a Merocyanine Dye Bound to Sulfonatocalixarenes: Effect of pH and the Size of Macrocycle on the Kinetics

Zsombor Miskolczy and László Biczók*

Institute of Molecular Pharmacology, Research Centre for Natural Sciences, Hungarian Academy of Sciences, P.O. Box 17, 1525 Budapest, Hungary

ABSTRACT: The effect of 1:1 complex formation on the photochromic behavior of the merocyanine isomer of a nitro-substituted spirobenzopyran dye was studied in aqueous solution using 4-sulfonatocalixarene (SCXn) cavitands possessing four or eight phenol units. The binding constants were independent of the size of the macrocycle, and about 7-fold more stable associates were produced at pH 2.3 than in slightly alkaline solution. The complexation with SCXn diminished the acidity of protonated merocyanine (*trans*-MCH$^+$) and precluded its photoinitiated transition to spirobenzopyran form, but did not affect the reactions in basic media. Upon exposure to light, the complexed *trans*-MCH$^+$ was converted to cis isomer. The association with 4-sulfonatocalix[4]arene slowed down the thermal back reaction in the dark to a larger extent than the confinement to 4-sulfonatocalix[8]arene. Both the activation energy and the Arrhenius *A* factor were significantly larger when the smaller, more rigid macrocycle served as a host.

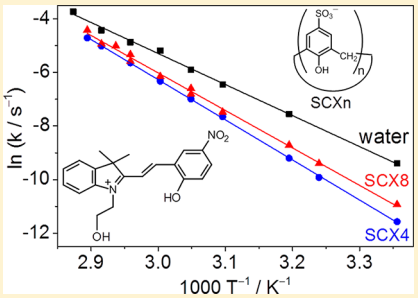

1. INTRODUCTION

The reversible interconversion between spirobenzopyrans and merocyanines has been extensively studied due to its numerous applications.[1−5] The equilibrium between the two photochromic forms is strongly solvent- and substituent-dependent.[6,7] Introduction of a nitro group in the 6-position of the benzopyran moiety shifts the equilibrium from the spiro toward the merocyanine isomer. Because of its large dipole moment,[8,9] the colored planar merocyanine form is stabilized by hydrogen bonding and dipole−dipole interactions in polar solvent,[10] whereas the closed colorless spiro form is usually thermodynamically more stable in apolar medium. Spiropyrans have been used for optical sensing of metal ions,[11−13] anions,[14,15] and amino acids.[16] The selective association between the membrane-bound merocyanine form with zwitterionic amino acid permits of the photocontrolled transfer of amino acid from the aqueous phase into the liposomal bilayer.[17] The entirely different binding properties of the two photochromic forms were exploited to control the association with DNA by light.[18] Reversible photoswitchable aptamer recognition was achieved by the selective binding of spiropyran to RNA oligonucleotide,[19] and photocontrol of enzyme activity was accomplished.[20] A spiropyran derivative was developed that had no significant effect on the cellular survival, but the intracellular photoisomerization to the merocyanine form induced a dramatic toxic response.[21]

The low solubility of the majority of photochromic compounds in water was circumvented by confinement in self-assembled systems, such as micelles,[22,23] vesicles,[24] and bile salt aggregates.[25] Cationic derivatives were synthesized to study the effects of inclusion in cucurbit[7]uril.[26] Spiropyrans showed little tendency for encapsulation in cyclodextrins in aqueous solution,[27] but complexation of the merocyanine form took place with γ-cyclodextrins in water−dimethy sulfoxide mixtures.[9] We have shown that both merocyanine and its protonated form produce a very stable inclusion complex with cucurbit[8]uril cavitand leading to enhanced chemical stability, improved solubility, and significantly altered photochromic behavior.[28] Using the smaller cucurbit[7]uril macrocycle, a preferential binding of the protonated merocyanine was observed, and the photoinduced transformation of this species to the spiropyran isomer was selectively accelerated.[29] As a continuation of these studies, now, we extend the investigations to 4-sulfonatocalixarenes (SCXn), the highly water-soluble macrocycles that are versatile building blocks in supramolecular chemistry.[30] Their π-electron-rich, flexible cavity composed of *n* 4-hydroxy-benzenesulfonate units linked by methylene groups can encapsulate a wide variety of organic compounds and cations.[31−34] We focus on the confinement of the photochromic forms of *N*-(2-hydroxyethyl)-3′,3′-dimethyl-6-nitrospiro[2*H*-1-benzopyran-2,2′-indoline], which can be applied in molecule-based logic circuits, optical signal switches, and molecular machines.[35−38] Our main goal is to reveal how the cavity size and pH influence the kinetics of the merocyanine−spiropyran interconversion in flexible anionic SCXn cavitands and the stability of the complexes. The studied reactions and the formula of the employed calixarenes are shown in Scheme 1. Several merocyanine isomers with dominating trans or cis characters exist in solution.[39,40] Scheme 1 displays the most probable trans and cis conformers participating in the

Received: October 15, 2012
Revised: November 26, 2012
Published: December 27, 2012

Scheme 1. Studied Reactions and Formula of 4-Sulfonatocalix[*n*]arenes

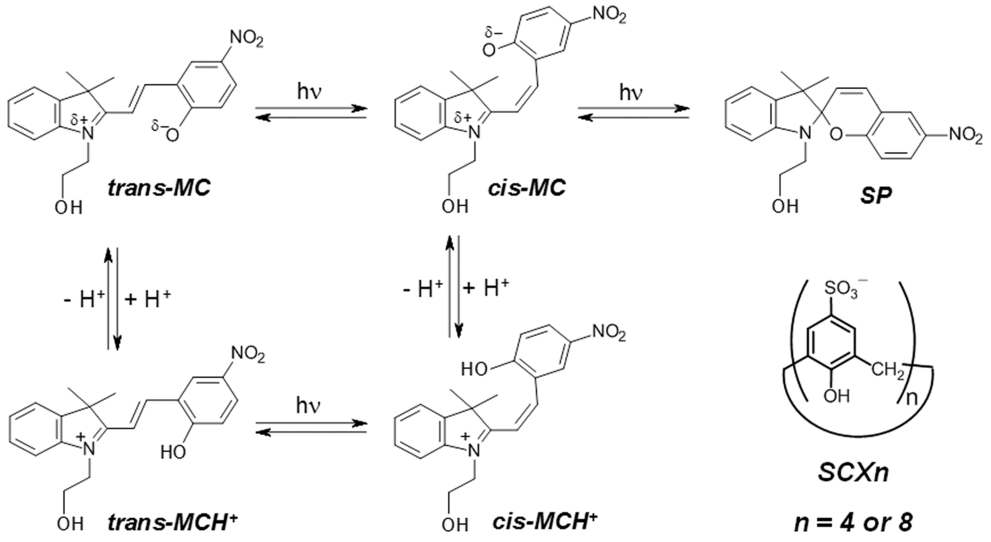

photochromic reactions, as suggested by quantum chemical calculations.[41]

2. EXPERIMENTAL SECTION

N-(2-Hydroxyethyl)-3′,3′-dimethyl-6-nitro-spiro[2*H*-1-benzopyran-2,2′-indoline] (SP) (TCI) was used without further purification. Aqueous solutions of MCH^+ and MC were prepared from SP as described previously.[28] 4-Sulfonatocalix[4]arene (SCX4) (Fluka) and 4-sulfonatocalix[8]arene (SCX8) (Acros Organics) held 1:9 and 1:21 stoichiometric amounts of water in their crystal structures.[42] The pH of the solutions, adjusted with HCl or KOH, was measured with Consort C832 equipment. The glass electrode was calibrated at pH 4, 7, and 10 with buffer standards. The UV−vis absorption spectra were recorded on a Unicam UV 500 or a Hewlett-Packard spectrophotometer. Corrected fluorescence spectra were obtained on a Jobin-Yvon Fluoromax-P spectrofluorometer. The samples were photolyzed using a 150 W xenon lamp and monochromator in a 1 cm × 0.4 cm quartz cell. The whole solutions were exposed to light. The temperature was controlled with a Julabo thermostat. The experimental data were analyzed by the ORIGINPRO8 software.

3. RESULTS AND DISCUSSION

3.1. Effect of SCXn on the Acidity of *trans*-MCH^+. In the ground state, *trans*-MCH^+ is the thermodynamically most stable photochromic form in acidic aqueous solution below pH 3 due to its significant stabilization by interaction with solvent molecules.[10] Gradual addition of KOH leads to color change from yellow to orange-red indicating that the deprotonation of the phenolic OH group produces *trans*-MC. In this species, the lone electron pair of the negatively charged oxygen participates in the extended conjugation in the ground state but the dipole moment substantially diminishes in the first singlet-excited state.[9] Figure 1 displays the emergence of *trans*-MC absorbance at 505 nm as a function of pH. As a representative example, the inset shows the absorption spectra in the presence of 0.77 mM SCX4 at pH 2.84 and 7.38. The experimental results were analyzed by nonlinear least-squares fit of the following function:

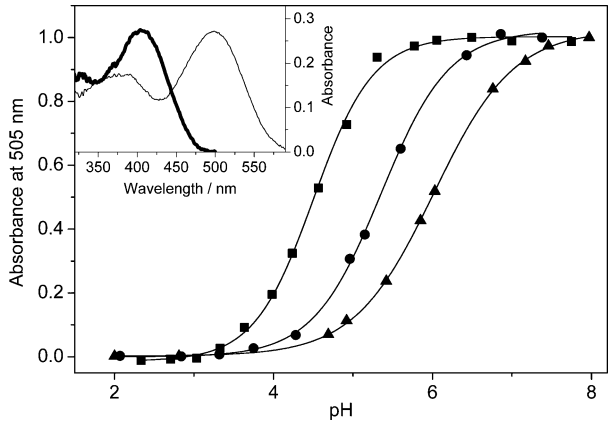

Figure 1. Variation of the normalized absorbance of 0.016 mM *trans*-MCH^+ solution at 505 nm as a function of pH in the presence of 0.77 mM SCX4 (●), 0.79 mM SCX8 (▲), and in water (■). The lines represent the results of the nonlinear least-squares fit of eq 1 to the experimental data. Inset displays the absorption spectra in 0.77 mM SCX4 solution at pH 2.84 (thick line) and 7.38 (thin line).

$$A = \frac{A_0 - A_\infty}{1 + \exp[(\mathrm{pH} - \mathrm{p}K_a)/P]} + A_\infty \quad (1)$$

where pK_a represents the negative logarithm of the equilibrium constant of the proton dissociation from *trans*-MCH^+, $P = 1/\ln 10$, whereas A_0 and A_∞ are the absorbances at low and high pHs, respectively. A marked shift of the titration curve toward less acidic range was observed in the presence of SCX4, while the bulkier SCX8 macrocycle brought about even larger displacement. The pK_a values were found to be 4.52, 5.35, and 6.02 in water, SCX4, and SCX8 complex, respectively. The estimated uncertainty of the calculated pK_a values is ±0.04. The interaction with the anionic hosts impeded the proton loss of *trans*-MCH^+ because this cationic form had larger binding affinity than the uncharged *trans*-MC. The larger negative charge of SCX8 hindered the proton removal more efficiently bringing about thereby more significant pK_a enhancement than the complexation with SCX4.

It is worth noting that the interaction with SCXn did not alter the kinetics of *trans*-MC decomposition, the process taking place above pH 8.[29,43] This is in sharp contrast to the

dx.doi.org/10.1021/jp310167j | J. Phys. Chem. B 2013, 117, 648−653

behavior of the dye in cucurbit[8]uril cavity, where the nucleophilic addition of OH^- to *trans*-MC is inhibited by the considerable negative charge density of the carbonyl-rimmed portal of the host.[28] The more open structure of SCXn cannot provide protection against the attack of OH^- to the 2-position of the heterocyclic ring of *trans*-MC.

3.2. Determination of the Binding Constants. The sulfonic acid moieties of SCXn are completely dissociated above pH 0.4. The pK_a's of the gradual deprotonation of the phenolic OH groups are reported to be 3.44, 4.26, 7.78, and 10.3 for SCX8, whereas they are 3.28 and 11.5 for SCX4 in the presence of 0.1 M NaCl.[44] Somewhat larger pK_a values were found at lower ionic strength.[44] We examined the complexation of *trans*-MCH^+ at pH 2.3 to ensure that only the sulfonic acid moieties of the hosts lose protons. The studies with *trans*-MC were performed at pH 7.6–8.0, where only one OH at the lower rim of SCX4 was deprotonated and the majority of SCX8 macrocycles had two phenolate groups.

Figure 2 shows the absorbance and fluorescence intensity variations as a function of SCX8 concentration at pH 2.3,

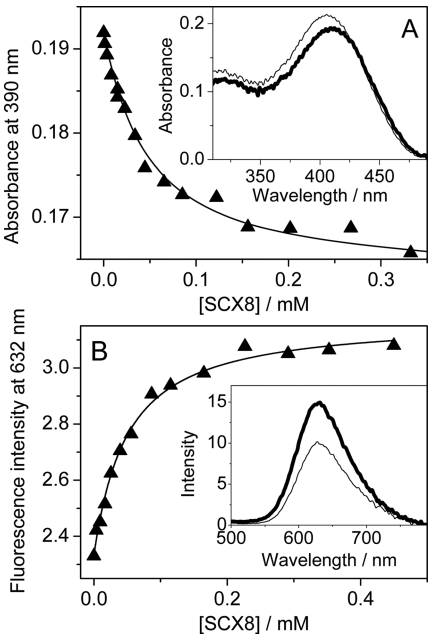

Figure 2. (A) Absorbance change of 0.012 mM *trans*-MCH^+ at 390 nm and (B) fluorescence enhancement in 0.0065 mM *trans*-MCH^+ aqueous solution at 632 nm at pH 2.3 upon addition of SCX8. The lines display the results of the global nonlinear least-squares analysis (see text). Insets: (A) absorption spectra in the presence of 0 and 0.20 mM SCX8; (B) fluorescence spectra in the presence of 0 and 0.75 mM SCX8 (excitation at 428 nm).

whereas the insets depict the spectra of the uncomplexed and bound *trans*-MCH^+. The slight hypochromicity and the bathochromic shift of the absorption maximum from 406 to 410 nm are evidence for complex formation. The considerable displacement of the fluorescence maximum relative to the absorption band is attributed to the rapid proton release from *trans*-MCH^+ in the singlet-excited state since the spectrum corresponds to that found upon excitation of *trans*-MC (vide infra). Complex formation with SCX8 produces negligible change in the shape and position of the fluorescence band, but causes 36% fluorescence intensity enhancement. Fluorescence increase upon inclusion in SCXn is rare[45,46] because electron transfer from SCXn to the singlet-excited guest usually results in efficient quenching. Such a process cannot occur in excited *trans*-MCH^+–SCX8, because (i) electron transfer cannot compete with the fast photoinduced deprotonation generating singlet-excited *trans*-MC–SCX8 and (ii) the dye in the latter species is a weak electron acceptor due to its uncharged character and low excited-state energy.

The change of the fluorescence intensity (I) with the total SCX8 concentration ($[SCX8]_0$) could be described well by the function derived for 1:1 binding with an equilibrium constant K:[47]

$$I = I_0 + \frac{I_\infty - I_0}{2}\left\{1 + \frac{[SCX8]_0}{[dye]_0} + \frac{1}{K[dye]_0} - \left[\left(1 + \frac{[SCX8]_0}{[dye]_0} + \frac{1}{K[dye]_0}\right)^2 - 4\frac{[SCX8]_0}{[dye]_0}\right]^{1/2}\right\} \quad (2)$$

where $[dye]_0$ is the initial dye concentration and I_∞ and I_0 stand for the fluorescence intensities of the complexed and free dyes. The global nonlinear least-squares analysis of the fluorescence data provided $K = (2.2 \pm 0.3) \times 10^4\ M^{-1}$. Similar treatment of the absorbance data in the 300–500 nm range resulted in $K = (2.5 \pm 0.5) \times 10^4\ M^{-1}$. Considering the slight absorbance alteration upon *trans*-MCH^+–SCX8 formation (Figure 2A), the agreement between the K values derived from fluorescence and spectrophotometric titrations are fair, and the fluorescence titration is deemed more accurate method.

The nonionic *trans*-MC had considerably lower binding affinity to SCX8 as seen from the association constants listed in Table 1. The absorption spectrum of *trans*-MC at pH 7.6 did

Table 1. Equilibrium Constants of Complex Formation of the Photochromic Species with SCXn Derived from Fluorescence Titrations

	$K/10^3\ M^{-1}$	
	SCX8	SCX4
MCH^+	22 ± 0.3	25 ± 0.3
	25 ± 0.5[a]	
MC	3.2 ± 0.4	3.5 ± 0.4

[a]From absorbance change.

not alter even in the presence of 1 mM SCX8. However, the fluorescence intensity slightly diminished owing to *trans*-MC–SCX8 complex formation (Figure 3). Dynamic fluorescence quenching can be excluded because the fluorescence lifetime of *trans*-MC is shorter than 100 ps in water.[29]

When the smaller SCX4 served as a host, the binding of neither *trans*-MCH^+ nor *trans*-MC caused absorbance change, but the intensity of the fluorescence band decreased (Figure 4). The similar fluorescence spectra at pH 2.3 and 7.6 demonstrate the rapid photoinduced deprotonation in *trans*-MCH^+–SCX4. The binding constants (K) derived from the nonlinear least-squares fit of eq 2 to the experimental data are given in Table 1. Surprisingly, the K values are practically independent of the cavity size of the host. This suggests that the photochromic dye is not embedded deeply in the calixarene macrocycle. The larger stability of *trans*-MCH^+–SCXn complexes compared to that of *trans*-MC–SCXn associates indicates that electrostatic

dx.doi.org/10.1021/jp310167j | J. Phys. Chem. B 2013, 117, 648–653

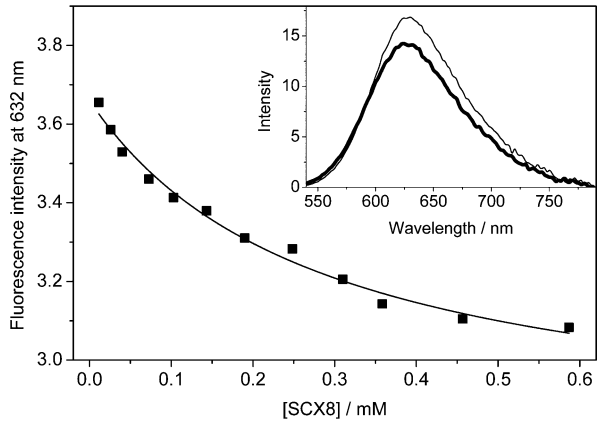

Figure 3. Fluorescence intensity diminution of 0.0065 mM *trans*-MC at 632 nm as a function of SCX8 concentration (excitation at 470 nm, pH 7.6). The line shows the result of the nonlinear least-squares fit of eq 2 to the experimental data. Inset: fluorescence spectra in the presence of 0 (thin line) and 0.77 mM SCX8 (thick line).

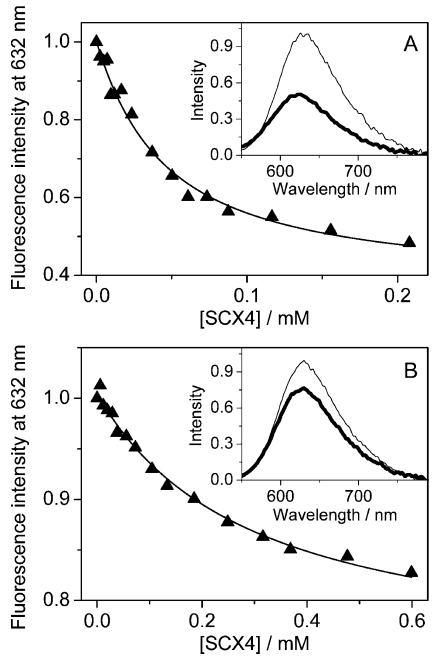

Figure 4. Effect of association with SCX4 on the fluorescence intensity alteration at 632 nm in photochromic dye solutions at pH 2.3 ($\lambda_{excitation}$ = 428 nm) (A) and pH 7.8 ($\lambda_{excitation}$ = 502 nm) (B). The lines give the results of the nonlinear least-squares fit of eq 2 to the plotted experimental data. Insets: fluorescence spectra for uncomplexed dye (thin line) and SCX4 complex (thick line) at pH 2.3 (A) and 7.8 (B).

forces between host and guest significantly contribute to the binding affinity. The low solubility of the dye thwarted the determination of the structure of the complexes by NMR spectroscopy.

3.3. Photochromic Reactions of SCXn Complexes at pH 2.3. The yellow color of *trans*-MCH$^+$−SCXn solutions gradually fades during irradiation with 410 nm light. As a representative example, the inset to Figure 5 presents the absorption spectrum before and after photolysis in the case of SCX8 host. Analogous spectra are recorded using SCX4. For the sake of comparison, the absorption of the spiropyran (SP) form, the species produced from free *trans*-MCH$^+$ upon exposure to light, is also displayed. The spectra clearly show

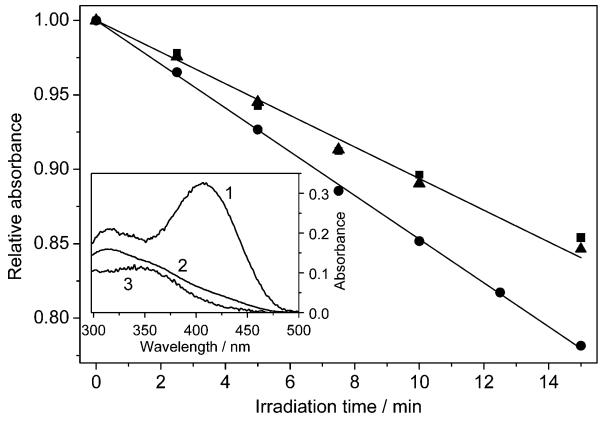

Figure 5. (A) Relative absorbance variation of 0.017 mM *trans*-MCH$^+$ during irradiation with 410 nm light in the absence of additive (■) and in the presence of 0.81 mM SCX8 (▲) and 0.85 mM SCX4 (●) at pH 2.3. The lines were obtained by linear least-squares fit. Inset: absorption spectra at pH 2.3 before (1) and after photolysis (2) of 0.050 mM *trans*-MCH$^+$ and 0.37 mM SCX8 solution (optical path 4 mm). SP absorption spectrum in water (3).

that the photoproduct is not SP. The shape and maximum of the absorption band of the photoproduct are analogous to those of the *cis*-MCH$^+$−cucurbit[8]uril inclusion complex.[28] Thus, we can conclude that *trans*-MCH$^+$−SCXn undergoes photoisomerization leading to *cis*-MCH$^+$−SCXn. The interaction with SCXn blocks the deprotonation of *cis*-MCH$^+$ just like the inclusion in the cucurbit[8]uril cavity. Since the loss of proton is indispensable for the closure of the spiro ring (Scheme 1), the complexed *cis*-MCH$^+$ cannot be transformed into SP. The trans−cis photoisomerization was followed by absorbance measurements at 406 nm. The initial reaction rate was independent of temperature, but markedly differed for SCX4 and SCX8 complexes. As seen in Figure 5, the association with the smaller macrocycle accelerated the photoisomerization by ca. 44%, whereas the reactions of SCX8-bound and free *trans*-MCH$^+$ had practically the same kinetics. For the closely related *N*-methyl derivative, Görner demonstrated that the trans−cis photoisomerization takes place predominantly from the singlet-excited state via an intermediate possessing perpendicular conformation.[48]

The thermal back isomerization from *cis*- to *trans*-MCH$^+$ in SCXn complex followed first-order kinetics (inset to Figure 6). The rise of absorbance (A) at 410 nm was analyzed with the relationship:

$$A = A_\infty - (A_\infty - A_0)e^{-kt} \quad (3)$$

where t denotes the reaction time and A_0 and A_∞ are the initial and final absorbances. Nonlinear least-squares fit of the experimental results at 298 K gave $k = (1.8 \pm 0.1) \times 10^{-5}$ and $(9.8 \pm 0.5) \times 10^{-6}$ s^{-1} for the rate constant of the back reaction from *cis*-MCH$^+$−SCX8 and *cis*-MCH$^+$−SCX4, respectively. To gain more insight into the effects controlling the kinetics of isomerization, temperature-dependent measurements were carried out. Figure 6 presents the Arrhenius plots of the rate constant of cis−trans isomerization in SCXn complex and, for the sake of comparison, the rate constant of the transformation of free SP to *trans*-MCH$^+$. The calculated pre-exponential factors (A) and activation energies (E_A), obtained by nonlinear least-squares fit, are summarized in Table 2. Since the back reactions to *trans*-MCH$^+$ are not

dx.doi.org/10.1021/jp310167j | J. Phys. Chem. B 2013, 117, 648−653

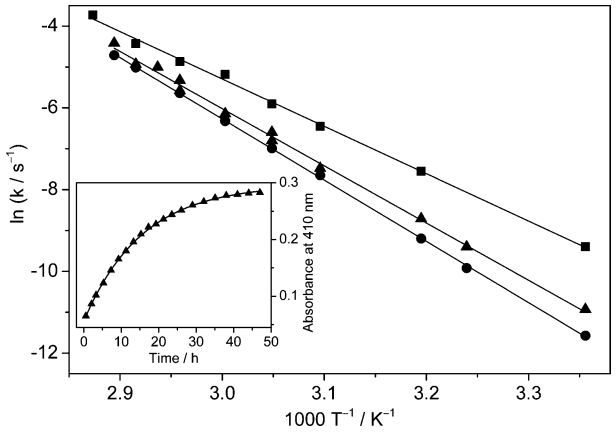

Figure 6. Arrhenius plot of the rate constants of the thermal back reactions in the presence of 0.85 mM SCX4 (●), 0.81 mM SCX8 (▲), and in the absence of additive (■) at pH 2.3. Inset: representative example of the absorbance rise at 410 nm due to back formation of *trans*-MCH$^+$−SCX8 in the dark at 298 K and the fitted line according to eq 3 (pH 2.3).

Table 2. Arrhenius Parameters of the Thermal Back Reactions from the Photoproduct to *trans*-MCH$^+$ at pH 2.3

photoproduct	E_A/kJ mol^{-1}	A/s^{-1}
uncomplexed SP	96 ± 2	(6 ± 3) × 10^{12}
cis-MCH$^+$−SCX8	116 ± 2	(4 ± 2) × 10^{15}
cis-MCH$^+$−SCX4	124 ± 2	(6 ± 2) × 10^{16}

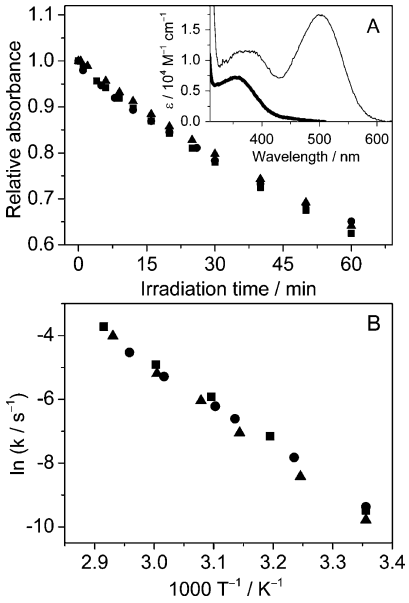

Figure 7. (A) Relative absorbance variation of 0.013 mM *trans*-MC at 506 nm during irradiation light above 480 nm in the absence of additive (■) and in the presence of 0.83 mM SCX8 (▲) and 0.78 mM SCX4 (●) at pH 8.0. Inset: absorption spectra at pH 8.0 before (thin line) and after (thick line) photolysis in the presence of SCX8. (B) Arrhenius plot of the rate constants of SP transformation to *trans*-MC in the dark in 0.87 mM SCX4 (●) and 0.82 mM SCX8 (▲) solutions and in the absence of additive (■) at pH 8.0.

elementary processes, A and E_A should be considered as empirical parameters. Despite the fact that the opening of the spiro ring precedes the isomerization in the absence of SCXn, lowest E_A is found in neat water. Quantum chemical calculations demonstrated that the cleavage of the spiro ring in water requires much lower activation energy than cis−trans isomerization.[41] The binding to SCX8 augments E_A by 20 kJ mol^{-1}, whereas a further 8 kJ mol^{-1} E_A increase takes place for the SCX4 complex. The association with macrocycles impedes cis−trans isomerization in the ground state due to steric reasons. The more rigid SCX4 represents larger steric hindrance than the conformationally mobile SCX8, which can easily adapt itself to the geometrical features of the guest. Thus, more energy is required to initiate conformation change when *cis*-MCH$^+$ is bound to SCX4. The Arrhenius A factor exhibits parallel increase with E_A. The large A factors of the *cis*-MCH$^+$−SCXn → *trans*-MCH$^+$−SCXn reactions imply substantial positive activation entropy. The isomerization goes through a transition state in which the components are looser bound than in the initial complex. The reaction of SCX4 complex possesses considerably larger A factor than that of SCX8 because a more substantial increase in the degrees of freedom is feasible upon passage to the transition state when the process starts from the complex of the more rigid SCX4 macrocycle.

3.4. Photochromic Reactions of SCXn Complexes at pH 8.0. When *trans*-MC−SCXn is exposed to light above 480 nm at pH 8.0, the orange-red color of the solution vanishes. The absorption spectrum of the photoproduct agrees with that obtained in the photolysis of free *trans*-MC, which is known to generate SP. The weak binding of the dye to SCXn (vide supra) does not prevent the closure of the spiro ring after trans−cis photoisomerization. Figure 7A displays the spectra before and after light exposure together with the relative absorbance variation in the course of photoreaction at 506 nm. The gradual disappearance of MC has the same kinetics in water and in SCXn complex. The initial rate of the reactions does not vary with temperature.

The thermal back formation of *trans*-MC from SP is a first-order process with *cis*-MC intermediate. The Arrhenius plot of the rate constants determined at various temperatures is presented in Figure 7B. In contrast to the findings at pH 2.3, negligible difference is obtained among the Arrhenius parameters of SP → *trans*-MC transformation in water and in SCXn complexes. The E_A = 107 ± 9 kJ mol^{-1} and A = (5.8 ± 1.7) × 10^{14} s^{-1} values of this process are significantly smaller than the corresponding parameters for the *cis*-MCH$^+$−SCXn → *trans*-MCH$^+$−SCXn isomerization listed in Table 2. The difference indicates that the looser binding of the uncharged SP and *cis*-MC to SCXn hinders the structural alteration to a lesser extent and, consequently, less activation energy is needed for the isomerization. Moreover, the weaker host−guest interactions restrict the movement of the constituents to a lesser extent. Therefore, less entropy gain is attained in the transition states when the structural rearrangement starts from the looser-bound SP−SCXn complex compared to the back isomerization of the stronger-bound *cis*-MCH$^+$−SCXn.

4. CONCLUSIONS

The binding to the highly negative flexible SCXn cavitands changes the photochromic characteristics completely differently from that observed previously for cucurbiturils. In the case of the latter hosts, the equilibrium constant of 1:1 complex formation of *trans*-MCH$^+$ significantly increases with growing cavity size, but the strength of the association with SCXn is found to be independent of the number of phenol units in the macrocycle. This suggests that *trans*-MCH$^+$ is not included

dx.doi.org/10.1021/jp310167j | J. Phys. Chem. B 2013, 117, 648−653

deeply in SCXn, and hydrophobic interactions play less role in the stabilization of *trans*-MCH$^+$−SCXn. The considerably lower binding affinity of uncharged *trans*-MC indicates the importance of electrostatic forces in *trans*-MCH$^+$−SCXn formation. In contrast to the protection of *trans*-MC against decomposition by inclusion in cucurbit[8]uril, the dye remains accessible to nucleophilic attack by OH^- in SCXn complexes. Because of its substantial negative charge, SCXn efficiently hinders the deprotonation of the bound guests. This effect enhances the pK_a of *trans*-MCH$^+$ and blocks the spiro isomer formation from *cis*-MCH$^+$ by photoinduced ring closure. The thermal back conversion of *cis*-MCH$^+$ to trans form has lower Arrhenius parameters in CB8 than in water due probably to the effect of the nonpolar microenvironment in the cavity of CB8. Contrarily, the association with SCXn significantly increases both the activation energy and *A* factor of the process. SCXn barely alters the polarity around the dye but sterically impedes cis−trans isomerization. Since SCXn affects the photochromic transformations only in acidic solution, the effect of SCXn can be reversibly controlled with pH alteration. For this purpose, the utilization of SCX4 is the most advantageous because it promotes the trans−cis photoisomerization and efficiently stabilizes *cis*-MCH$^+$ at pH 2.3.

AUTHOR INFORMATION

Corresponding Author

*Fax: +36-1-438-1143. E-mail: biczok.laszlo@ttk.mta.hu.

Notes

The authors declare no competing financial interest.

ACKNOWLEDGMENTS

The authors very much appreciate the support of this work by the Hungarian Scientific Research Fund (OTKA, Grant K104201).

REFERENCES

(1) Paramonov, S. V.; Lokshin, V.; Fedorova, O. A. *J. Photochem. Photobiol., C* **2011**, *12*, 209−236.
(2) Berkovic, G.; Krongauz, V.; Weiss, V. *Chem. Rev.* **2000**, *100*, 1741−1753.
(3) Mistlberger, G.; Crespo, G. A.; Xie, X.; Bakker, E. *Chem. Commun.* **2012**, *48*, 5662−5664.
(4) Kosa, T.; Sukhomlinova, L.; Su, L.; Taheri, B.; White, T. J.; Bunning, T. J. *Nature* **2012**, *485*, 347−349.
(5) Hammarson, M.; Andersson, J.; Li, S.; Lincoln, P.; Andréasson, J. *Chem. Commun.* **2010**, *46*, 7130−7132.
(6) Chibisov, A. K.; Görner, H. *J. Phys. Chem. A* **1997**, *101*, 4305−4312.
(7) Görner, H. *Phys. Chem. Chem. Phys.* **2001**, *3*, 416−423.
(8) Bletz, M.; Pfeifer-Fukumura, U.; Kolb, U.; Baumann, W. *J. Phys. Chem. A* **2002**, *106*, 2232−2236.
(9) Burke, K.; Riccardi, C.; Buthelezi, T. *J. Phys. Chem. B* **2012**, *116*, 2483−2491.
(10) Shiraishi, Y.; Itoh, M.; Hirai, T. *Phys. Chem. Chem. Phys.* **2010**, *12*, 13737−13745.
(11) Zhu, J. F.; Yuan, H.; Chan, W. H.; Lee, A. W. M. *Org. Biomol. Chem.* **2010**, *8*, 3957−3964.
(12) Natali, M.; Giordani, S. *Org. Biomol. Chem.* **2012**, *10*, 1162−1171.
(13) Chibisov, A. K.; Görner, H. *Chem. Phys.* **1998**, *237*, 425−442.
(14) Shao, N.; Wang, H.; Gao, X.; Yang, R.; Chan, W. *Anal. Chem.* **2010**, *82*, 4628−4636.
(15) Shiraishi, Y.; Itoh, M.; Hirai, T. *Tetrahedron Lett.* **2011**, *52*, 1515−1519.
(16) Shao, N.; Jin, J. Y.; Cheung, S. M.; Yang, R. H.; Chan, W. H.; Mo, T. *Angew. Chem., Int. Ed.* **2006**, *45*, 4944−4948.
(17) Sunamoto, J.; Iwamoto, K.; Mohri, Y.; Kominato, T. *J. Am. Chem. Soc.* **1982**, *104*, 5502−5504.
(18) Andersson, J.; Li, S.; Lincoln, P.; Andréasson, J. *J. Am. Chem. Soc.* **2008**, *130*, 11836−11837.
(19) Young, D. D.; Deiters, A. *ChemBioChem* **2008**, *9*, 1225−1228.
(20) Aizawa, M.; Namba, K.; Suzuki, S. *Arch. Biochem. Biophys.* **1977**, *180*, 41−48.
(21) Nilsson, J. R.; Li, S. M.; Onfelt, B.; Andréasson, J. *Chem. Commun.* **2011**, *47*, 11020−11022.
(22) Favaro, G.; Ortica, F.; Malatesta, V. *J. Chem. Soc., Faraday Trans.* **1995**, *91*, 4099−4103.
(23) Ikeda, S.; Saso, Y. *Colloids Surf.* **1992**, *67*, 21−27.
(24) Ishiwatari, T.; Kondo, T.; Mitsuishi, M. *Colloid Polym. Sci.* **1996**, *274*, 1000−1005.
(25) Li, R.; Santos, C. S.; Norsten, T. B.; Morimitsu, K.; Bohne, C. *Chem. Commun.* **2010**, *46*, 1941−1943.
(26) Nilsson, J. R.; Parente Carvalho, C.; Li, S.; Da Silva, J. P.; Andréasson, J.; Pischel, U. *ChemPhysChem* **2012**, *13*, 3691−3699.
(27) Zhou, J. W.; Sui, Q.; Huang, B. H. *J. Photochem. Photobiol., A* **1998**, *117*, 129−136.
(28) Miskolczy, Z.; Biczók, L. *J. Phys. Chem. B* **2011**, *115*, 12577−12583.
(29) Miskolczy, Z.; Biczók, L. *Photochem. Photobiol.* **2012**, *88*, 1461−1466.
(30) Atwood, J. L.; Barbour, L. J.; Hardie, M. J.; Raston, C. L. *Coord. Chem. Rev.* **2001**, *222*, 3−32.
(31) Guo, D.-S.; Wang, K.; Liu, Y. *J. Inclusion Phenom. Macrocyclic Chem.* **2008**, *62*, 1−21.
(32) Megyesi, M.; Biczók, L. *J. Phys. Chem. B* **2010**, *114*, 2814−2819.
(33) Miskolczy, Z.; Biczók, L. *Chem. Phys. Lett.* **2009**, *477*, 80−84.
(34) Perret, F.; Lazar, A. N.; Coleman, A. W. *Chem. Commun.* **2006**, 2425−2438.
(35) Raymo, F. M.; Giordani, S. *J. Am. Chem. Soc.* **2001**, *123*, 4651−4652.
(36) Raymo, F. M.; Giordani, S.; White, A. J. P.; Williams, D. J. *J. Org. Chem.* **2003**, *68*, 4158−4169.
(37) Raymo, F. M.; Giordani, S. *J. Am. Chem. Soc.* **2002**, *124*, 2004−2007.
(38) Silvi, S.; Arduini, A.; Pochini, A.; Secchi, A.; Tomasulo, M.; Raymo, F. M.; Baroncini, M.; Credi, A. *J. Am. Chem. Soc.* **2007**, *129*, 13378−13379.
(39) Ernsting, N. P.; Arthen-Engeland, T. *J. Phys. Chem.* **1991**, *95*, 5502−5509.
(40) Gahlmann, A.; Lee, I. R.; Zewail, A. H. *Angew. Chem., Int. Ed.* **2010**, *49*, 6524−6527.
(41) Sheng, Y.; Leszczynski, J.; Garcia, A. A.; Rosario, R.; Gust, D.; Springer, J. *J. Phys. Chem. B* **2004**, *108*, 16233−16243.
(42) Yang, W.; Villiers, M. M. d. *Eur. J. Pharm. Biopharm.* **2004**, *58*, 629−636.
(43) Stafforst, T.; Hilvert, D. *Chem. Commun.* **2009**, 287−288.
(44) Suga, K.; Ohzono, T.; Negishi, M.; Deuchi, K.; Morita, Y. *Supramol. Sci.* **1998**, *5*, 9−14.
(45) Dsouza, R. N.; Pischel, U.; Nau, W. M. *Chem. Rev.* **2011**, *111*, 7941−7980.
(46) Megyesi, M.; Biczók, L. *Chem. Phys. Lett.* **2006**, *424*, 71−76.
(47) Valeur, B. *Molecular Fluorescence, Principles and Applications*; Wiley-VCH: Weinheim, Germany, 2002.
(48) Görner, H.; Atabekyan, L. S.; Chibisov, A. K. *Chem. Phys. Lett.* **1996**, *260*, 59−64.